J. Cosmet. Sci., **61,** 147–160 (March/April 2010)

18-MEA and hair appearance

HIROTO TANAMACHI, SHINICHI TOKUNAGA,
NORIYUKI TANJI, MASASHI OGURI, and SHIGETO INOUE,
Beauty Research Center, Kao Corporation, 2-1-3, Bunka, Sumida-ku, Tokyo 131-8501 (H.T., S.T.), Analytical Science Research Laboratories, Kao Corporation, 2606 Akabane, Ichikai, Haga, Tochigi 321-3497 (M.O.), and Analytical Science Research Laboratories, Kao Corporation, 1334 Minato, Wakayama-shi, Wakayama, 640-0112 (N.T., S.I.), Japan.

Accepted for publication August 13, 2009.

Synopsis

The effects of the removal of 18-MEA on the dynamic contact angle (advancing contact angle and receding contact angle) and friction force (friction force microscopy (FFM)) were examined in the present study. Chemically untreated hair tresses formed more finely ordered bundles, with the fibers aligned more parallel to each other, in the wet state, and lying flat and aligned parallel to each other in the dry state. Hair tresses in which 18-MEA had been removed by potassium t-butoxide treatment formed coarser tangled bundles and were aligned in a disorderly manner in the wet state, causing the hair to become entangled and disorderly in the dry state. This was because the 18-MEA-removed hair fibers adhered to each other and were not easy to realign in the wet state. The distorted part of the bundle dried faster and the tress shape was eventually fixed in the entangled shape. One role of 18-MEA is to allow hair fibers to lie flat and parallel with respect to each other in the wet state by providing relatively high receding contact angles and low surface friction. Hair alignment in the dry state is directly affected by hair alignment in the wet environment, particularly in the case of damaged hair.

INTRODUCTION

Healthy and beautiful hair is of interest to many females who have had their hair damaged by chemical processing, heat styling, and environmental factors. There are a lot of aspects that are required to make hair beautiful, of which the following three points are essential. The first is appearance: shine, luster and high contrast. The second is hair alignment, silhouette and how the hair moves; i.e., whether hair fibers can move smoothly and separately, e.g., when the wind blows. The third is texture: a silky and smooth feel. It seems very important that each of these attributes has to be present to some degree to provide beautiful hair.

The cuticle forms the outer surface of the hair fiber, protecting the cortex. The cuticle consists of flat overlapping cells that are attached at the root end and point toward the tip end of the hair fibers, like tiles on a roof. The shape and orientation of the cuticle cells are responsible for the differential friction effect in hair (1). The outermost surface of the

cuticle cells has been suggested to be covered by a layer of covalently bound fatty acids, a major component of which is 18-methyleicosanoic acid (18-MEA). 18-MEA is an unusual branched-chain fatty acid, covalently bound, via thioester or ester linkages, to the cuticle surface of hair fibers (2–5). The absence of 18-MEA is considered one of the reasons for an increase in interfiber friction, and it may have an influence on sensory perceptions of hair, such as a dry feel and difficult combing (6).

For decades, many studies have been made to investigate the roles of 18-MEA on the surface properties of hair. FFM is a powerful technique for the investigation of surface properties, including wetting and tribological properties, and has revealed that 18-MEA makes the surface hydrophobic and acts as a boundary lubricant to decrease frictional resistance (6–10). Dynamic contact angle measurement is another useful method to examine the changes in surface hydrophobicity and has indicated that when 18-MEA is removed, the surface of hair becomes hydrophilic (11–14). In this study, we have investigated the effects of the removal of 18-MEA on the surface properties in wet and dry environments and the role of 18-MEA on hair alignment and appearance.

EXPERIMENTAL

MATERIALS

Hair samples. Hair fibers, kindly provided by 48 Japanese females, were cut at the root end, just above the scalp. Twenty-three subjects had chemically untreated hair, and the hair of the others had been treated by bleaching, coloring, and/or permanent waving.

The hair fibers for our specific experiment were kindly provided by a Japanese female aged 40. The fibers were cut at a distance of approximately 20 cm from the root end on the back of her head. The hair had never been treated with any chemical agents, such as bleaches, hair coloring, or permanent-waving solutions.

Preparation of 18-MEA-removed hair. The hair fibers were treated with a solution of 0.1 M potassium t-butoxide in t-butanol for five minutes at room temperature and at a liquor:fiber ratio of 10:1. The alkali was then removed by rinsing the hair with t-butanol (2×), ethanol, and finally, by washing in water.

METHODS

Semi-quantitative analysis of 18-MEA. Semi-quantitative analysis of 18-MEA adsorbed on the outermost surface of the hair fiber was measured by a TOF-SIMS IV instrument (ION-TOF GmbH, Germany) using 25-keV Bi_3^{2+} primary ions (average current 0.13 pA, pulse width 23.0 ns, repetition rate 10 kHz) in high-current bunched mode. The analysis area of 50 × 50 μm was randomly rastered by primary ions and was charge-compensated by low-energy electron flooding. The amount of 18-MEA was expressed as the relative ion yield of 18-MEA versus the CN ion yield, which was derived from hair proteins. It is known that the ion yield of 18-MEA detected by TOF-SIMS changes under the influence of not only the amount of 18-MEA on the surface of the hair but also sample conditions, surface charging, and instrument condition. For the comparison of the ion yield of 18-MEA among samples, the peak was generally normalized by the standard ion peak,

such as the sum of the total ion yield, the ion peak from hydrocarbons, or the ion peak from the matrix constituent. In the case of using the sum of the total ion yield or the ion peak from hydrocarbons as a standard ion, however, these yields change due to surface contaminants such as anionic surfactants and silicone oil. Here, the ion peak from the matrix constituent was chosen as a standard ion to avoid these effects. In this study, the CN ion was used for normalization since the matrix of the hair surface is keratinous protein and the CN ion was strongly detected in the TOF-SIMS measurement of hair samples.

Measurement of surface properties of hair. The wetting forces of hair were measured by the Wilhelmy method using a K100MK2 tensiometer (Kruss). Single hair fibers were scanned over 3 mm at a velocity of 2 mm/min for the advancing mode. Dynamic contact angles were calculated from

$$F = \pi d \gamma \cos\theta$$

where F is the wetting force, d is the diameter of the hair, γ is the surface tension of water, and θ is the contact angle of the liquid versus the fiber surface. The hair fiber diameter was measured on the transverse section of each fiber with a rotating fiber diameter measurement system equipped with a laser (Kato Tech Co.) at 20°C and at a relative humidity (RH) of 65%. The wetting force measurements were also performed at 20°C, 65% RH.

Frictional properties of the outermost surface of the hair in the wet environment were measured using a Nanoscope III Dimension 3000 (Veeco Instruments, Santa Barbra, CA). Friction force microscopy (FFM) data were acquired using unmodified silicon nitride (Si-N) cantilevers (spring constant of 0.12 Nm^{-1}). After engagement of the tip with the cuticle surface, the tip was scanned parallel to the longitudinal axis of the fiber. In order to minimize scanning artifacts, a scan rate of 1 Hz was used for all measurements. To characterize frictional properties, 2- × 2-μm scans of the cuticle faces (without edges) were performed. Trace and retrace FFM datasets were obtained, and the friction force was calculated by subtracting the retrace FFM signal from the trace FFM signal. In the FFM measurement of the cuticle surfaces before and after removing 18-MEA, trace and retrace FFM datasets were obtained at different areas of the cuticle surfaces; samples were randomly picked up from untreated hair and 18-MEA-removed hair, and trace and retrace FFM datasets were obtained.

RESULTS AND DISCUSSION

INFLUENCE OF SCALE DIRECTION OF HAIR ON DYNAMIC CONTACT ANGLE

A sensitive method to provide information on the outermost surface of hair is contact angle measurement. Its interpretation, however, is not always straightforward because surfaces usually give two stable contact angles, advancing and receding. The difference between the advancing and receding contact angles is referred to as contact angle hysteresis. It is generally accepted that the contact angle hysteresis can be due to a multitude of effects, such as surface roughness, chemical heterogeneity, surface deformation, and surface configuration changes (15–19).

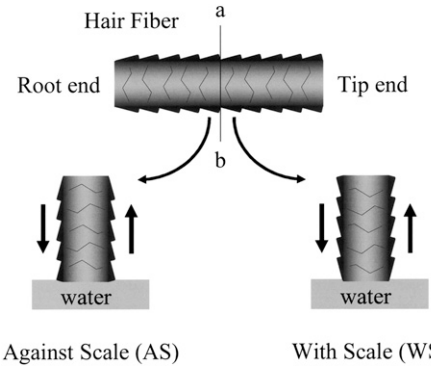

Figure 1. Schematic description of the method for studying the effect of the scale direction of hair on dynamic contact angle measurements.

In the case of the dynamic contact angle measurements, it is necessary to take the scale direction of the hair into account because cuticle cells are attached at the root end and point forward toward the tip end of the hair fiber. In order to examine the scale direction, a single hair fiber was cut vertically into two pieces along the line a–b in Figure 1, and the dynamic contact angles were measured by immersing the resulting cut areas in water.

Figure 2 shows the typical force curves for untreated hair in the "against scale" (AS) and "with scale" (WS) directions. Figure 3 shows the advancing and receding contact angles for untreated hair in the AS and WS directions. The error bar of each column represents the standard deviation within each group. The asterisk symbol in Figure 3 indicates a significant *p*-value obtained from Student's *t*-test. There was a significant difference in the receding contact angles between the AS and WS directions while there was no significant difference in the advancing contact angles between the AS and WS directions. The receding contact angle for untreated hair was higher in the WS direction than in the AS direction. The results agreed with those of Molina *et al*. (13) and Kamath *et al*. (20). Kamath *et al*. explained their reasons for the receding contact angles for untreated hair being higher in the WS direction than in the AS direction as follows: in the receding mode the frontal edges of the scales provide a lower contact angle (possibly due to scale edge abrasion) in the AS direction, while the dorsal sides of the scales, which are hydrophobic due to the presence of 18-MEA, make a greater contribution in the WS direction, which is

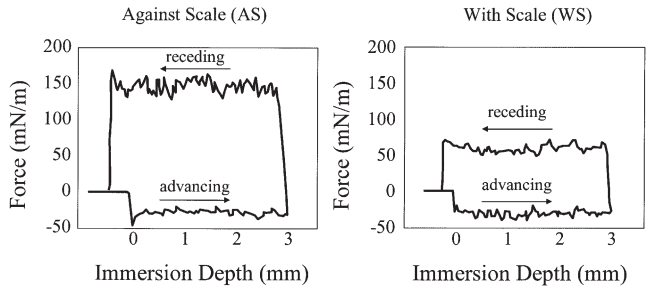

Figure 2. Typical contact angle force curves for untreated hair in the "against scale" (AS) and "with scale" (WS) directions.

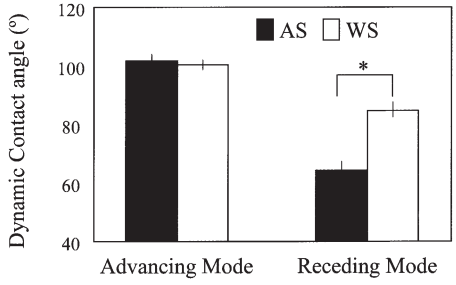

Figure 3. Advancing and receding contact angles for untreated hair in the "against scale" (AS) and "with scale" (WS) directions. The bars represent means for n=5; the whiskers represent the standard deviations. The asterisk symbol indicates the *p*-value obtained from Student's *t*-test; $*p < 0.001$.

illustrated in Figure 4 (20). Figure 5 shows the schematic description of a hair fiber, illustrating the dorsal side versus the frontal side. The frontal side is the edge of the cuticle, which is hydrophilic, most likely, due to removal of 18-MEA by abrasion and scale chipping exposing the hydrophilic materials below the epicuticle. The aim of the present study was to identify the roles of 18-MEA on hair appearance, and so the WS direction was chosen for the dynamic contact angle measurements of the hair fibers.

SURFACE PROPERTIES OF HAIR IN A WET ENVIRONMENT

Each fiber was washed with a plain shampoo (15wt% of sodium polyoxyethylene lauryl ether sulfate (2.5 E.O.) with 2wt% N, N-bis(2-hydroxyethyl)-dodecanamide solution adjusted to pH7 with phosphoric acid) and cut at 5-cm intervals from the root end to the tip. Then, the relative ion yield of 18-MEA versus the CN ion yield on the outermost surface of the hair, dynamic contact angles, and friction force microscopy were measured.

Advancing contact angle is the surface property that is related to the water wettability of hair fibers going from a dry to a wet environment. Receding contact angle is the surface

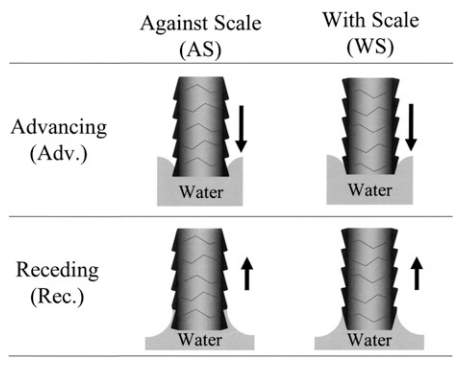

Figure 4. Explanation for the receding contact angles for untreated hair being higher in the WS direction than that in the AS direction. In the receding mode the frontal edges of the scales influence a lower contact angle in the AS direction while the dorsal sides of the scales make a greater contribution in the WS direction, as proposed by Kamath *et al.* (20).

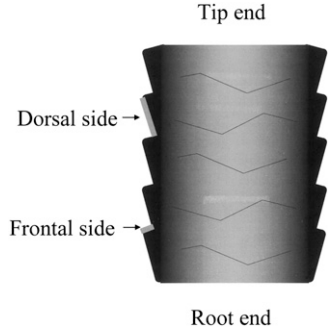

Figure 5. Schematic description of a hair fiber illustrating the dorsal vs the frontal side. The frontal side is the edge of the cuticle, which is more hydrophilic due to the hydrophilic materials below the 18-MEA layer.

property that is related to the drainage of hair fibers during the drying process, going from a wet to a dry environment. Figure 6 shows the relationship between dynamic contact angles (advancing and receding) and the relative ion yield of 18-MEA versus the CN ion yield on the outermost surface of hair measured by TOF-SIMS. Squares represent the advancing contact angle and triangles represent the receding contact angle. A decrease in 18-MEA led to a decrease in both the advancing contact angle and the receding contact angle. In the case of the advancing contact angle, there were two stages in this decrease: First, when the relative ion yield of 18-MEA versus the CN ion yield decreased to 0, the advancing contact angle decreased gradually from 120° to around 100°. The correlation coefficient (R) and *p*-value (p) for the slope of the line were obtained by regression analysis. R was 0.76 and p was 4.0×10^{-29} (n=149). A strong correlation between the advancing contact angle and the relative ion yield of 18-MEA versus the CN ion yield was observed. The slope of the approximated line for the advancing contact angle was 58.31.

In the second stage, after the relative ion yield of 18-MEA versus the CN ion yield reached 0, the advancing contact angle decreased drastically from around 100° to below

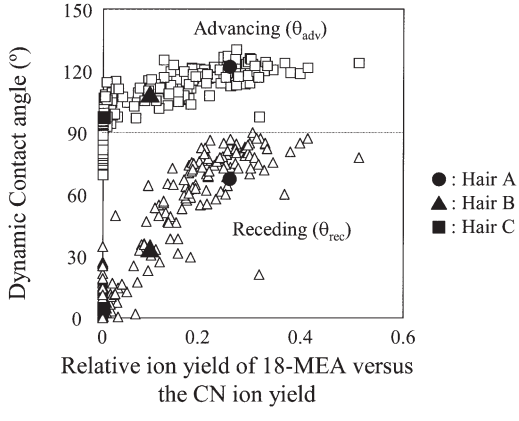

Figure 6. Dynamic contact angle vs the relative ion yield of 18-MEA versus the CN ion yield plot. The white squares represent the advancing contact angle and the white triangles represent the receding contact angle. Hair A, hair B, and hair C are selected for friction force investigations.

Table I
Relative Ion Yield of 18-MEA vs the CN Ion Yield and Dynamic Contact Angles of Hair

		Hair A	Hair B	Hair C
Relative ion yield of 18-MEA vs the CN ion yield		0.27	0.10	0.00
Contact angles	Advancing	121.4°	113.3°	99.5°
	Receding	65.1°	33.7°	6.1°

70°. It was very interesting that the surface of the hair maintained some degree of hydrophobicity even after removal of most of the 18-MEA. The receding contact angle, on the other hand, decreased in a linear manner from 80° to 0° as the relative ion yield of 18-MEA versus the CN ion yield decreased to 0. The correlation coefficient (R) and *p*-value (p) for the slope of the regression line were also obtained. R was 0.92 and p was 4.0×10^{-99} (n=237). A strong correlation between the receding contact angle and the relative ion yield of 18-MEA versus the CN ion yield was observed. The slope of the line for the receding contact angle, 251.96, was 4.3 times larger than that of the advancing contact angle, 58.31. The results indicate that the decrease in 18-MEA on the cuticle surface affects the fibers more in going from a wet to a dry environment than in going from a dry to a wet environment.

In order to investigate the role of 18-MEA on the surface friction in the wet state, three hair fibers, hair A, hair B, and hair C (Figure 6), were selected, and friction force microscopy was performed. The surface properties of hair A, hair B, and hair C, are listed in Table I. In the FFM study, an unmodified silicon nitride (Si-N) AFM tip was used. The unmodified silicone nitride AFM tip (21) and hair surface are both hydrophilic in the wet state, although the components of these substances are different. It was hypothesized that the interaction between the AFM tip and the hair surface in the wet environment could thus correspond to the interaction between one hair fiber and another in the wet environment. To characterize friction properties, 2 μm × 2 μm scans of the cuticle surface (avoiding the edges) of the cuticle were performed. Figure 7 shows the typical FFM images for hair A, hair B, and hair C in water at 2-μm × 2-μm scan size. Darker areas represent the friction force as being lower, and brighter areas represent the friction force as being higher. The average values of the friction force for hair A, hair B, and hair C are shown in Figure 8. The bars represent means for n=6 areas of each fiber, and the whiskers represent the standard deviations. The asterisk symbol indicates the *p*-value obtained from analysis of variance (ANOVA). The relative ion yield indicated that most of the 18-MEA was removed for hair C and that it gave the highest friction value. The

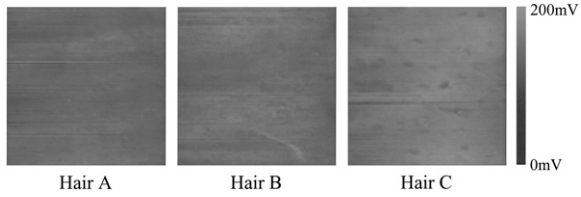

Figure 7. Typical FFM images for hair in water at 2-μm × 2-μm scan size. Darker areas represent a lower friction force and brighter areas represent a higher friction force.

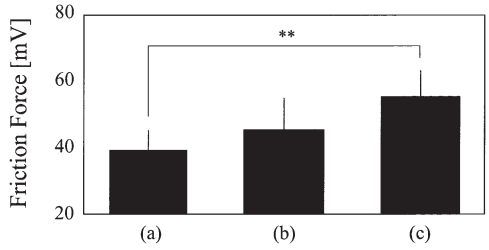

Figure 8. Friction forces for (a) hair A, (b) hair B, and (c) hair C in water. The bars represent means for n=6 areas of each fiber; the whiskers represent the standard deviations. The asterisk symbol indicates the *p*-value obtained from analysis of variance (ANOVA); $^{**}p < 0.01$.

results of ANOVA showed that there was a significant difference in the friction force between hair A and hair C. That means the decrease in 18-MEA led to an increase in the friction force in the wet state.

A decrease in 18-MEA also led to a decrease in the receding contact angle and an increase in friction force. One can picture the high frictional force as the strong adhesive force that causes the fiber aggregation. The combination of the decrease in the receding contact angle and the increase in the friction force in the wet environment should affect hair alignment in the wet state and make the hair fibers entangle more readily in the wet state.

Since some of the hair fibers examined here experienced a variety of damage, such as chemical damage, mechanical damage, and heat and sunlight, a lot of structural changes were observed on the surface of the hair: scale lifting, broken cuticle scale edges, removal of cuticle, and so on. It seemed difficult to identify the role of 18-MEA itself on hair alignment with these fibers. In order to determine the role of 18-MEA on hair alignment, 18-MEA-removed hair was prepared using chemically untreated hair, and it was investigated for the effects of the removal of 18-MEA on hair alignment.

ROLES OF 18-MEA ON HAIR APPEARANCE

It was necessary to check that the treatment by which 18-MEA is removed does not affect the physical properties of the hair fiber, except for the surface properties, since the aim of the present study was to determine the role of 18-MEA itself on hair alignment. Scanning electron microscopy (SEM) images of the hair surface, the diametric swelling ratio in water, the elastic modulus in water, and the breaking stress in water for chemically untreated hair and 18-MEA-removed hair were analyzed for this purpose (Table II). There were no significant differences in the SEM images between the untreated hair and 18-MEA-removed hair. There were also no significant differences in the diametric swelling ratio in water, the elastic modulus, and the breaking stress between the untreated hair and the 18-MEA-removed hair by Student's *t*-test. It was confirmed that the removal of 18-MEA did not change these properties, and therefore we concluded that this 18-MEA removal treatment affected only the fiber surface.

The relative ion yield of 18-MEA versus the CN ion yield on the outermost surface of hair and the contact angles for untreated hair and 18-MEA-removed hair are listed in Table III. The relative ion yield of 18-MEA versus the CN ion yield for untreated hair and

18-MEA-removed hair were 0.37 ± 0.14 and 0.00, respectively. The advancing contact angles for untreated hair and 18-MEA-removed hair were 102.9° ± 4.8° and 88.0° ± 4.8°, respectively. The receding contact angles for untreated hair and 18-MEA-removed hair were 60.0° ± 9.0° and 3.2° ± 5.5°, respectively. It was confirmed that 18-MEA on the outermost surface was essentially removed by this procedure. It was also confirmed that the

Table II
Structural and Physical Properties of Hair (n = 7)

	Untreated hair	18-MEA-removed hair
SEM image	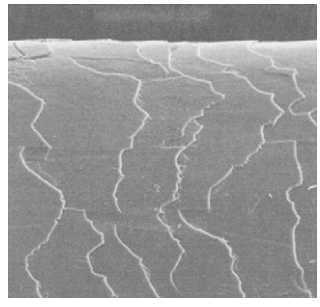	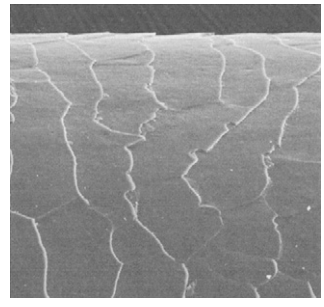
Diametric swelling ratio in water (%)	1.08 ± 0.02	1.08 ± 0.15
Elastic modulus in water ($\times 10^{10}$ dyns/cm^2)	1.77 ± 0.26	1.68 ± 0.53
Breaking stress in water ($\times 10^{9}$ dyns/cm^2)	1.75 ± 0.24	1.82 ± 0.24

Table III
The Relative Ion Yield of 18-MEA vs the CN Ion Yield and Contact Angles of Hair (n = 5)

		Untreated hair	18-MEA-removed hair
The relative ion yield of 18-MEA vs the CN ion yield		0.37 ± 0.14	0.00
Contact angles	Advancing	102.9° ± 4.8°	88.0° ± 4.8°
	Receding	60.0° ± 9.0°	3.2° ± 5.5°

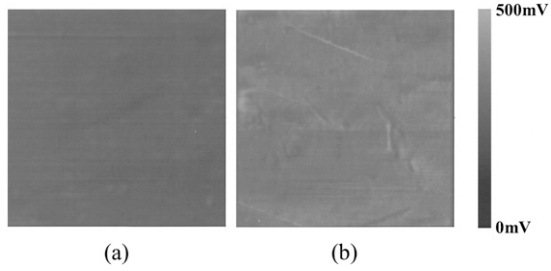

Figure 9. Typical FFM images for (a) untreated hair and (b) 18-MEA-removed hair in water at 2-μm × 2-μm scan size. Darker areas correspond to a lower friction force and brighter areas correspond to a higher friction force.

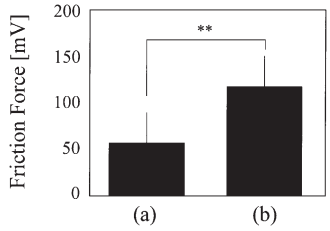

Figure 10. Friction forces of (a) untreated hair and (b) 18-MEA-removed hair in water. The bars represent means for n=5; the whiskers represent the standard deviations. The asterisk symbols indicate the *p*-values obtained from Student's *t*-test; $^{**}p < 0.01$.

reduction of 18-MEA led to a larger decrease in the receding contact angle, 60° to 3°, compared to that of the advancing contact angle, 103° to 88°. Figure 9 shows typical FFM images for untreated hair and 18-MEA-removed hair in water, and the average values of the friction force are shown in Figure 10. The bars represent means for n=5, and the whiskers represent the standard deviations. The asterisk symbol in Figure 10 indicates the *p*-value obtained from Student's *t*-test. There was a significant difference in the friction forces between untreated hair and 18-MEA-removed hair. The removal of 18-MEA led to an increase in friction forces in water.

Figure 11 shows schematic diagrams of hair interactions in the wet state. A higher receding contact angle and a lower friction force in the wet state allow untreated hair fibers to move more easily over each other and realign with each other. The fact that the removal of 18-MEA decreased the receding contact angle suggests that 18-MEA-removed hair will remain wet longer and create a stronger adhesive force between hair fibers and make the hair fibers tend to aggregate together in the wet state. The fact that 18-MEA-removed hair gave a higher friction value suggests that 18-MEA-removed hair will be easier to tangle. It was thus expected that the combination of the decrease in receding contact angle and the increase in the friction force in the wet environment for 18-MEA-removed hair will affect hair alignment adversely in the wet state.

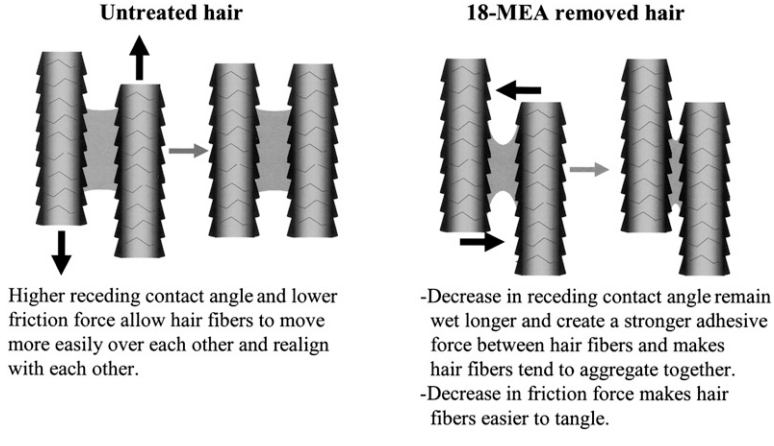

Figure 11. Schematic diagram of hair interactions in wet environment.

Figure 12. Shape of hair swatches in wet and dry states.

Figure 12 shows hair swatches for untreated hair and 18-MEA-removed hair in wet and dry states. 18-MEA-removed hair was entangled and aligned in a disorderly manner in the wet and dry states, while untreated hairs formed more ordered bundles and aligned more parallel with respect to each other in the wet state, and lay flat and aligned parallel to each other in the dry state. This was because the 18-MEA-removed hair fibers adhered more firmly to each other and, once the fibers were tangled, were not easy to realign. Hair alignment in the dry environment was directly affected by the hair alignment in the wet state, particularly in the case of damaged hair. Figure 13 and Figure 14 demonstrate schematic diagrams for the shape of hair swatches going from a wet to a dry state. Untreated hair fibers (Figure 13) form more ordered bundles and the fibers even align more parallel to each other in wet environments. The hair bundles separate into finer bundles during

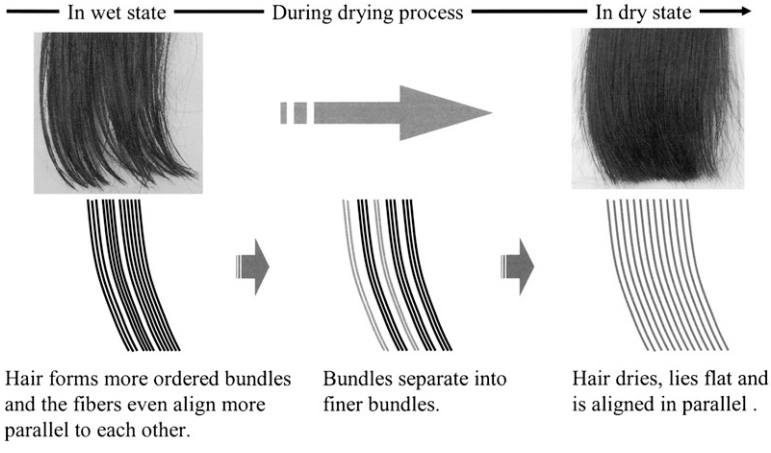

Figure 13. Schematic diagram of untreated hair going from a wet to a dry state.

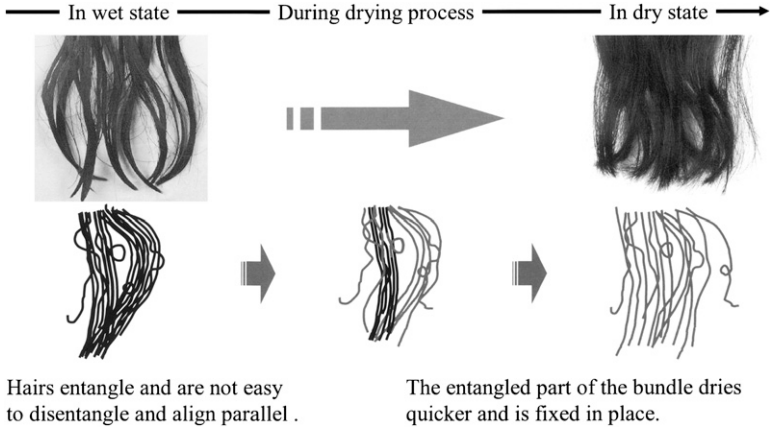

Figure 14. Schematic diagram of 18-MEA-removed hair going from a wet to a dry state.

the drying process. Then, the untreated dry hair fibers lie flat and align parallel to each other in the dry state. On the other hand, 18-MEA-removed hairs (Figure 14) entangle and are not easy to disentangle and align in a parallel manner. Then, the 18-MEA-removed hair fibers form coarser, tangled bundles, with disorderly alignment in the wet state. The entangled part of the bundle of the 18-MEA-removed hair dries quickly and is fixed in place.

Finally, light intensity measurements were performed in order to evaluate the effect of the removal of 18-MEA on the luminance along the hair tresses. Hair tresses were mounted on a cylinder, 4 cm in diameter. Digital images of the hair tresses were captured with a Nikon D50 digital camera, with a resolution of 3 megapixels, using a flash. Image analysis was carried out by scanning across highlighted and dark areas of the resultant image, using originally developed analysis software that enabled us to obtain the light intensity (luminance) distribution. Figure 15 provides example images of the hair tresses and light

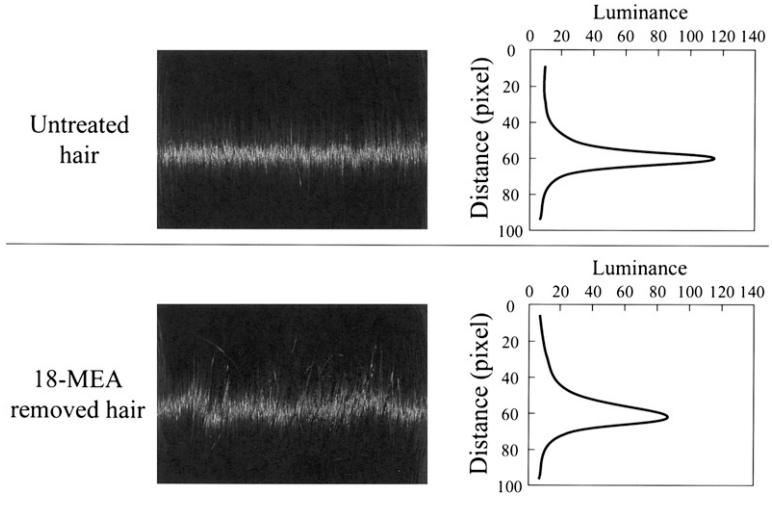

Figure 15. Images of hair tresses and light distribution curves for untreated hair and 18-MEA-removed hair.

distribution curves for untreated hair and 18-MEA-removed hair. It was apparent that the removal of 18-MEA decreases the contrast between specular reflection and other regions, which is due to the disorderly alignment of the hair fibers. Broadening of specular reflection, a luminance intensity of 88 and 18 pixels of half bandwidth, and approximately a 20% decrease in luminance intensity were evident in the case of 18-MEA-removed hair, while the specular reflection of the untreated hair was relatively sharp, having a luminance intensity of 115 and ten pixels of half bandwidth. The results revealed that the removal of 18-MEA decreases hair gloss.

CONCLUSIONS

The decrease in 18-MEA on the cuticle surface affects the hydrophobic–hydrophilic properties of hair by providing lower advancing and receding contact angles. An important cosmetic role of 18-MEA is to allow hair fibers to lie flat and parallel with respect to each other in wet environments by providing relatively high receding contact angles and low surface friction. Hair alignment in the dry environment, which influences hair luster, is directly affected by hair alignment in the wet environment, particularly in the case of damaged hair.

REFERENCES

(1) C. R. Robbins, *Chemical and Physical Behavior of Human Hair,* 4th ed. (Springer-Verlag, New York, 2002).
(2) A. P. Negri, H. J. Cornell, and D. E. Rivett, The nature of covalently bound fatty acids in wool fibers, *Aust. J. Agric. Res.,* **42,** 1285–1292 (1991).
(3) A. P. Negri, H. J. Cornell, and D. E. Rivett, Effects of proceeding on the bound and free fatty acid levels in wool, *Text. Res. J.,* **62,** 381–387 (1992).
(4) S. Naito, M. Ooshika, N. Yorimoto, and Y. Kuroda, The structure of bound lipids of human hair fibers and its physical properties, *Proc. 9th Int. Wool Text. Res. Conf., Biella, Italy,* **II,** 367–374 (1996).
(5) D. J. Evans and M. Lanczki, Cleaavage of integral surface lipids of wool by aminolysis, *Textile Res. J.,* **67,** 435–444 (1997).
(6) S. Breakspear, J. R. Smith, and G. Luengo, Effect of the covalently linked fatty acid 18-MEA on the nanotribology of hair's outermost surface, *J. Struct. Biol.,* **149,** 235–242 (2005).
(7) V. Dupres, T. Camesano, D. Langevin, A. Checco, and P. Guenoun, Atomic force microscopy imaging of hair: Correlations between surface potential and wetting at the nanometer scale, *J. Colloid Interface Sci.,* **269,** 329–335 (2004).
(8) V. Dupres, D. Langevin, P. Guenoun, A. Checco, G. Luengo, and F. Leroy, Wetting and electrical properties of the human hair surface: Delipidation observed at the nanoscale, *J. Colloid Interface Sci.,* **306,** 34–40 (2007).
(9) U. Kalkbrenner, H. Koener, H. Hoecker, and D. E. Rivett, Studies on the composition of the wool cuticle, *Proc. 8th Int. Wool Text. Res. Conf., Christchurch, New Zealand,* **I,** 398–407 (1990).
(10) M. Huson, D. Evans, J. Church, S. Hutchinson, J. Maxwell, and G. Corino, New insights into the nature of the wool fibre surface, *J. Struct. Biol.,* **163,** 127–136 (2008).
(11) Y. K. Kamath, C. J. Dansizer, and H.-D. Weigmann, Wettability of keratin fiber surfaces, *J. Soc. Cosmet. Chem.,* **28,** 273–284 (1977).
(12) T. Baba, N. Nagasawa, H. Ito, O. Yaida, and T. Miyamoto, Changes in the covalently bound surface lipid layer of damaged wool fibers and their effects on surface properties, *Textile Res. J.,* **71,** 308–312 (2001).
(13) R. Molina, F. Comelles, M. R. Julia, and P. Erra, Chemical modifications on human hair studies by means of contact angle determination, *J. Colloid Interface Sci.,* **237,** 41–46 (2001).
(14) R. A. Lodge and B. Bhushan, Wetting properties of human hair by means of dynamic contact angle measurement, *J. Appl. Polym. Sci.,* **102,** 5255–5265 (2006).

(15) R. E. Johnson, Jr. and R. H. Dettre, Contact angle hysteresis. III. Study of an idealized heterogeneous surface, *J. Phys. Chem.,* **68,** 1744–1750 (1964).
(16) Y. L. Chen, C. A. Helm, and J. N. Israeachvili, Molecular mechanisms associated with adhesion and contact angle hysteresis of monolayer surfaces, *J. Phys. Chem.,* **95,** 10736–10747 (1991).
(17) J. C. Berg, *Wettability,* Surfactant Science Series 49 (Marcel Dekker, New York, 1993).
(18) A. Marmur, Contact angle hysteresis on heterogeneous smooth surfaces, *J. Colloid Interface Sci.,* **168,** 40–46 (1994).
(19) O. N. Tretinnikov and Y. Ikeda, Dynamic wetting and contact angle hysteresis of polymer surfaces studies with the modified Wilhelmy balance method, *Langmuir,* **10,** 1606–1614 (1994).
(20) Y. K. Kamath, C. J. Dansizer, and H.-D. Weigmann, Wetting behavior of human hair fibers, *J. Appl. Polym. Sci.,* **22,** 2295–2306 (1978).
(21) B. Bhushan, Nanoscale characterization of human hair and hair conditioners, *Prog. Mat. Sci.,* **53,** 585–710 (2008).